Electronic Supplementary Material (ESI) for Dalton Transactions.

Supporting Information

Mechanistic Insight into Pb^{2+} and Hg^{2+} Ions Sensing using Cobalt-based Coordination Polymer in Aqueous Phase

Akashdeep Nath, [a] Diti Vikram Gaikwad [a] and Sukhendu Mandal [a]*

[a] School of Chemistry, Indian Institute of Science Education and Research Thiruvananthapuram, Thiruvananthapuram, Kerala-695551, India, E-mail: sukhendu@iisertvm.ac.in

Contents

A. Comparison table

Table S1. Literature of inorganic-organic hybrid materials-based Pb (II) sensors.

Sl. No.	Materials	Detection limit (M)	K_{sv} (M^{-1})	Interaction type	Turn-on/off	Ref.
1	[Co(BTB)(4,4'-azopyridine)].H_2O.DMF	7.08(±0.08) × 10^{-8}	2.2 × 10^4	Excited-state	Turn-off	This Work
2	[Eu_2(FDC)$_3$DMA(H_2O)$_3$].DMA.4.5 H_2O	8.2 ×10^{-6}	2.97 ×10^4	Excited-state	Turn-on	S1
3	CDs/QDs@ZIF-8	2.4 × 10^{-9}	8.46 ×10^4	Excited-state	Turn-off	S2
4	[Tb(ppda)(npdc)$_{0.5}$(H_2O)$_2$]$_n$	9.44 × 10^{-5}	1.05 × 10^5	Excited-state	Turn-on	S3
5	[Tb(L)(H_2O)$_5$]$_n$ (H_2L= 3,5-dicarboxyphenolate)	3.4 × 10^{-7}	1.75 × 10^4	Ground-state	Turn-off	S4
6	MOF-5-NH_2	2.5 × 10^{-7}	~2.8×10^2	Ground-state	Turn-off	S5
7	Cd(II)-MOF	1.9 × 10^{-9}	2.4 ×10^4	Ground-state	Turn-off	S6
8	Zn(II)-MOF	8 × 10^{-7}	1.18 ×10^4	Ground-state	Turn-off	S7
9	MOF-5	2 ×10^{-9}	-	Ground-state	Turn-on	S8
10	[Zn(Nptp)(HBTC)]$_n$	-	3.2 ×10^3	Ground-state	Turn-off	S9
11	In-MOF	3.14 ×10^{-8}	9.78 ×10^3	Ground-state	Turn-off	S10

B. EXPERIMENTAL SECTION

Chemicals. Cobalt chloride ($CoCl_2$), 1,3,5-Tris(4-carboxyphenyl) benzene, 4,4'-azopyridine, KCl, $CaCl_2$, $SrCl_2$, $MgCl_2$, $CuCl_2$, $ZnCl_2$, $MnCl_2$, $CoCl_2$ were procured from Sigma-Aldrich. LiCl, NaCl, $BaCl_2$, $NiCl_2$, $HgCl_2$, and $PbCl_2$ were bought from Finar Chemicals, Merck, SRL Pvt. Ltd., Alfa Aesar, and Spectrochem Pvt. Ltd., respectively. (***Caution: Lead chloride and mercury chloride are highly toxic****. High precaution and lab safety should be taken care while performing all the experiments with $Pb^{2+}$and Hg^{2+}. Being potentially dangerous to the environment, all the waste products after experiments should be treated with proper protocol).* p-Terphenyl was purchased from TCI Chemicals. Anhydrous *N, N'*-dimethylformamide (DMF), and HPLC cyclohexane were acquired from Spectrochem Pvt. Ltd. We used all the chemicals without any further purification. Double distilled water was used wherever required throughout the project.

Synthesis of 1 [Co(BTB)(4,4'-azopyridine)].(DMF)(H_2O). 0.25 mmol $CoCl_2$, 0.05 mmol 1,3,5-Tris(4-carboxyphenyl) benzene, 0.1 mmol 4,4'-azopyridine were measured in a 20 mL glass vial and dissolved with 7 mL H_2O, followed by 3 mL DMF and subjected to sonication for 1 h. The resulting solution mixture was kept in a 100 ^{0}C hot air oven for 2 days and allowed to cool down normally to room temperature. Orange-coloured flake-like crystals were formed, which were washed 3-4 times with DMF, dried under vacuum, and stored in an ambient condition for further experiments.

Single Crystal X-ray Diffraction. A good quality single-crystal was mounted at 170 K on a Rigaku Oxford Diffraction XtaLAB Synergy-S diffractometer combined with a HyPix-6000HE Hybrid Photon Counting (HPC) detector. We used Cu Kα (λ = 1.54184 Å) from PhotonJet micro-focus sealed X-ray Source. CrystAlisPro software suite was utilized for data processing.[S11] The computing structure was refined with full-matrix least-squares techniques using SHELXL 2018/3 (Sheldrick, 2015).[S12] All the hydrogens were positioned geometrically, whereas non-hydrogens atoms were refined anisotropically in OLEX2.[S13] Thermal constraints were used for disorderd DMF molecule.

General instrumentations. The powder X-ray diffraction (5 ^{0} < 2θ < 50 ^{0}) was carried out in Bruker D8 Advance X-ray diffractometer. The steady-state spectroscopy was performed on UV-2600 SHIMADZU UV-Vis/NIR spectrometer and Horiba Jobin Yvon Fluorolog-3 spectrofluorometer for absorption and emission, respectively. Thermal stability was obtained in a SDT Q600 (Shimadzu) analyzer at a heating rate of 10 °C/min from room temperature to 600 °C under a constant N_2 flow. Dynamic light scattering experiment was carried out in a Malvern Zetasizer Nano-ZS analyzer. The FT-IR spectra were measured in a SHIMADZU IRPrestige-21 spectrometer using KBr pellet.

Quantum yield calculation. We used p-terphenyl (in cyclohexane) as a reference for quantum yield measurement. We excited the BTB linker, **1**, and reference at 290 nm by keeping the individual absorbance similar (0.03-0.04). The relative quantum yield (ϕ_S) was measured after integrating the area of the emission spectra using the following equation,

$$\phi_S = \phi_R \left(\frac{I_S}{I_R}\right)\left(\frac{A_R}{A_S}\right)\left(\frac{n_S}{n_R}\right)^2 \qquad \text{..... (S1)}$$

where, *I* is an integrated area of the emission spectrum, *A* denotes absorbance, *n* is the refractive index of the solvent used (water for linkers and **1**, cyclohexane for p-terphenyl).[S14] ϕ_R is 0.93 when excited at 290 nm in cyclohexane.[S15]

Time-resolved fluorescence spectroscopy. The lifetime decay profile was measured using a 310 nm laser diode excitation source using time-correlated single-photon counting (TCSPC) technique on a

Horiba Jobin Yvon-IBH time-resolved fluorimeter, containing Hamamatsu R3809U-50 microchannel plate detector (instrument response time is 38.6 ps), coupled to a monochromator (5000M) and TCSPC electronics (Data station Hub including Hub-NL, NanoLED controller). DAS6.3 fluorescence decay analysis software was used to fit the obtained data.

Fluorescence sensing.

Probe solution preparation. 1 mg of **1** was dissolved in 1.7 mL distilled water and sonicated for 30 min, followed by centrifugation at 10000 rpm for 6 min. 1.5 mL of the supernatant was taken from the solution and added to 1.5 mL of distilled water, which was used for further sensing studies.

Metal ion solutions preparation. All the metal ion solutions were prepared in an aqueous medium. We prepared 10^{-2} M $PbCl_2$ as a primary solution; other working $PbCl_2$ solutions were made by diluting it with distilled water. The final concentration of metal ion was calculated when dissolved it in a quartz cuvette containing 3 mL of **1** solution. We used the same concentration of metal ions (10^{-5} M) for comparative studies.

Limit of Detection (LOD). The fluorescence quenching was plotted with different Pb (II) ion concentrations and fitted linearly. The obtained slope from the linear fit was used to calculate the LOD value employing the following equations,

$$\text{Limit of detection} = \frac{3\sigma}{Slope} \qquad \text{..... (S2)}$$

$$\sigma = 100 \times (I_{SE}/I_0) \qquad \text{..... (S3)}$$

where, I_{SE} denotes standard error in emission measurement which is calculated from baseline measurement monitored at 357 nm (10 times), I is pristine emission intensity of the **1**.[S16]

Recyclability test. The material was washed thoroughly in water after use for Pb (II) sensing and centrifuged to discard the water. This process was repeated four times, followed by drying under a vacuum before reusing for the next cycle.

Theoretical calculation.

A density functional theory was carried out to optimize the ground-state and excited-state geometry of BTB molecule along with frequency calculation using a polarized double-zeta basis set (cc-pVDZ) with long-range-corrected hybrid functional (ωb97xd).[S17] The Los Alamos effective core potential (ECP) $LanL_2$-DZ for Pb and split valence cc-pVDZ basis set for Cl atom was used with ωb97xd functional for geometry optimization of $PbCl_2$ molecule.[S18-19] The time-dependent DFT calculation was carried out with the same level of theory using a polarizable continuum model (PCM) for an aqueous medium.[S20] We employed the following equation to calculate the stabilization energy (Δ E),

$$\Delta E = E_{BTB\text{-}PbCl2} - (E_{BTB} + E_{PbCl2}) \qquad \text{..... (S4)}$$

Gaussian 16 program package was used for all the calculations.[S21]

C. Crystal Structure description

Table S2. Crystallographic parameters of **1**.

Parameters	
CCDC number	2238686
Empirical formula	$C_{39}H_{26}CoN_5O_8$
Formula weight	751.58
Crystal System	Triclinic
Space Group	*P-1* (No. 2)
a (Å)	9.4934 (4)
b (Å)	12.7660 (4)
c (Å)	15.1031 (6)
α (°)	75.989 (3)
β (°)	80.082 (3)
γ (°)	71.663 (3)
Volume (Å^3)	1676.56 (12)
Z	2
Calculated density (mg/m^3)	1.489
Absorption coefficient (mm^{-1})	4.559
θ range (^{0})	3.032 to 67.051
Reflections collected	17702
Unique reflections	5912
Number of parameters	482
Goodness-of-fit on F^2	1.062
Final R indices [I > 2sigma(I)]	R_1 = 0.0622, wR_2 = 0.1685
R indices (all data)	R_1 = 0.0680, wR_2 = 0.1728
$R_1 = \Sigma\|\|F_0\| - \|F_c\|\|/ \Sigma\|F_0\|$; $wR_2 = \{[w(F_0^2 - F_c^2)^2]/ [w(F_0^2)^2]\}^{1/2}$; $w = 1/[\sigma^2 (F_0)^2 + (aP)^2 + bP]$; $P = [(F_0^2,0) + 2(F_c)^2]/3$, where a = 0.0929 and b = 2.98	

Table S3. Selected bond lengths (Å) of **1**.

Atom	Atom	Length/Å	Atom	Atom	Length/Å
Co1	O1	2.036 (3)	N1	C6	1.334 (5)
Co1	O4	2.007 (3)	N1	C24	1.343 (5)
Co1	O6	2.094 (3)	N4	N3	1.236 (5)
Co1	O2	2.399 (3)	N4	C33	1.437 (5)
Co1	N1	2.136 (3)	N5	C27	1.337 (5)
Co1	N5	2.156 (3)	N5	C15	1.338 (5)
O1	C35	1.267 (5)	N3	C17	1.435 (5)
O4	C35	1.253 (5)	O5	C9	1.205 (5)
O6	C32	1.256 (5)	C37	O7	1.38 (2)
O8	C9	1.328 (5)	N2	C19	1.574 (17)
O2	C32	1.254 (5)			

Table S4. Selected bond angles (^{0}) of **1**.

Atom	Atom	Atom	Angle/^{0}	Atom	Atom	Atom	Angle/^{0}
O1	Co1	O6	90.29 (11)	C27	N5	C15	117.6 (3)
O1	Co1	O2	147.27 (11)	C15	N5	Co1	121.2 (3)
O1	Co1	N1	87.38 (11)	N4	N3	C17	113.3 (3)
O1	Co1	N5	91.12 (11)	C27	N5	Co1	120.9 (3)
O4	Co1	O1	125.32 (12)	O6	C32	C34	119.0 (3)
O4	Co1	O6	143.78 (12)	O2	C32	O6	120.6 (4)
O4	Co1	O2	87.38 (11)	O2	C32	C34	120.2 (4)
O4	Co1	N1	90.69 (11)	O7	C37	N2	120 (2)
O4	Co1	N5	88.12 (12)	C6	N1	Co1	121.3 (2)
O6	Co1	O2	57.57 (10)	O4	C35	O1	123.1 (3)
O6	Co1	N1	98.14 (11)	O5	C9	O8	123.6 (4)
O6	Co1	N5	84.38 (12)	O5	C9	C22	123.1 (4)
N1	Co1	O2	91.04 (11)	C6	N1	C24	117.7 (3)
C35	O1	Co1	117.7 (2)	N2	C37	O7	127.5 (19)
C35	O4	Co1	171.0 (3)	C24	N1	Co1	121.0 (2)
C32	O6	Co1	96.7 (2)	N3	N4	C33	114.0 (3)
C32	O2	Co1	82.9 (2)				

Topological Analysis

```
################################
1:C37 H24 Co N4 O6, H2 O, C2 N O
################################
Topology for Co1
--------------------
Atom Co1 links by bridge ligands and has
Common vertex with                    R(A-A)       f
Co 1   -0.6426    1.4165    0.5670   (-1 1 0)    13.298A       1
Co 1    1.3574   -0.5835    0.5670   ( 1-1 0)    13.298A       1
Co 1    0.3574    1.4165   -0.4330   ( 0 1-1)    17.254A       1
Co 1    0.3574   -0.5835    1.5670   ( 0-1 1)    17.254A       1
Common edge with                      R(A-A)
Co 1    0.6426    0.5835    0.4330   ( 1 1 1)     3.953A       2
Co 1    0.6426   -0.4165    1.4330   ( 1 0 2)    14.771A       2
-------------------------
Structural group analysis
-------------------------

-------------------------
Structural group No 1
-------------------------
Structure consists of layers ( 1 1 1) with CoO6N4C37H24
Num. groups=1; Thickness=6.60; Min.Distance=8.174

Coordination sequences
----------------------
Co1:  1  2  3  4   5   6   7   8   9  10
Num   6 14 22 30  38  46  54  62  70  78
Cum   7 21 43 73 111 157 211 273 343 421
----------------------
TD10=421

Vertex symbols for selected sublattice
--------------------------------------
Co1 Point symbol:{3^3.4^10.5.6}
Extended point symbol:[3.3.3.4.4.4.4.4.4.4.4.4.4.5.6(4)]
Rings with types: [*.*.*.*.*.*.*.*.*.*.*.*.*.*.*]
--------------------------------------
Point symbol for net: {3^3.4^10.5.6}
6-c net; uninodal net
```

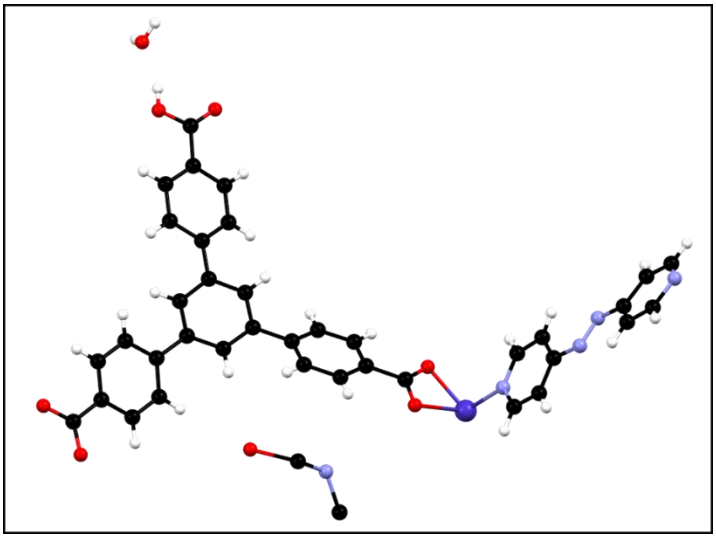

Fig. S1 Asymmetric unit of **1** (Co: Blue, C: Black, O: Red, N: Sky-blue, H: off-white).

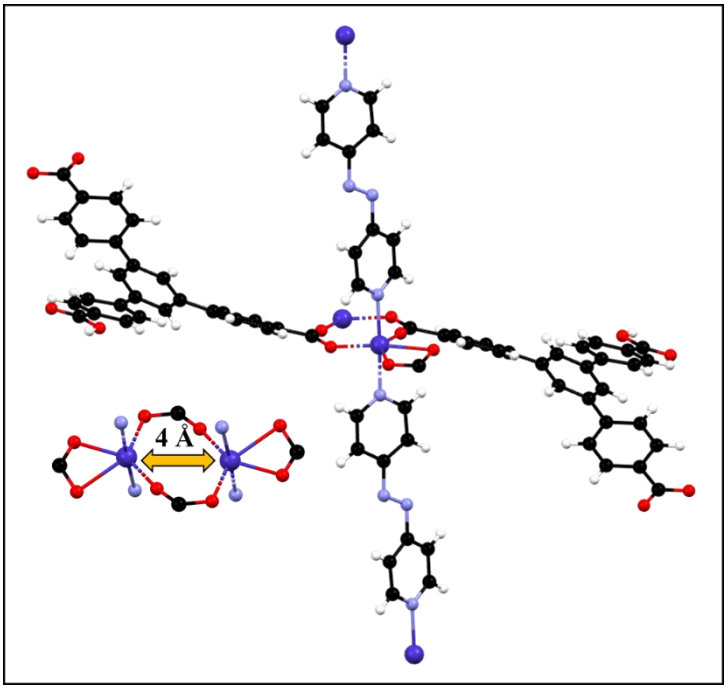

Fig. S2 Coordination pattern of Co (II) centre in framework (Co: Blue, C: Black, O: Red, N: Sky-blue, H: off-white).

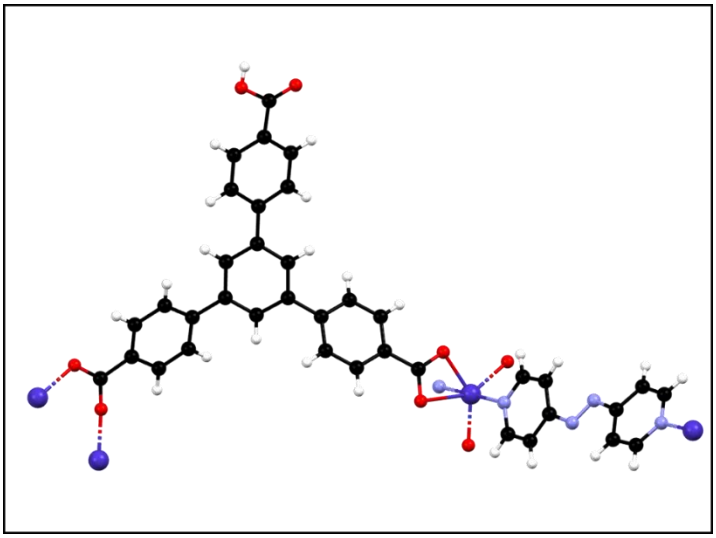

Fig. S3 Coordination mode of BTB in framework (Co: Blue, C: Black, O: Red, N: Sky-blue, H: off-white).

D. FT-IR spectra

(a)

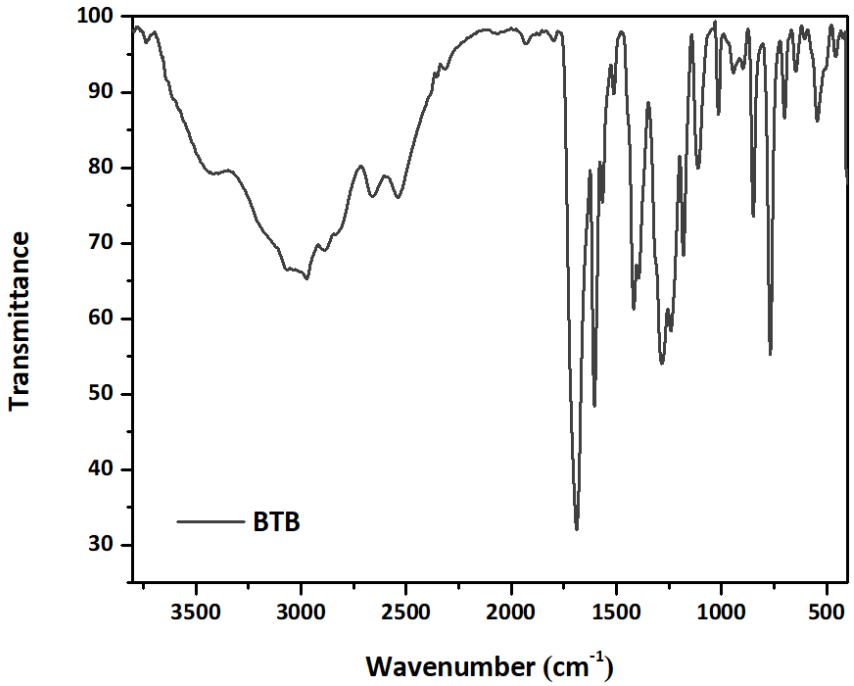

(b)

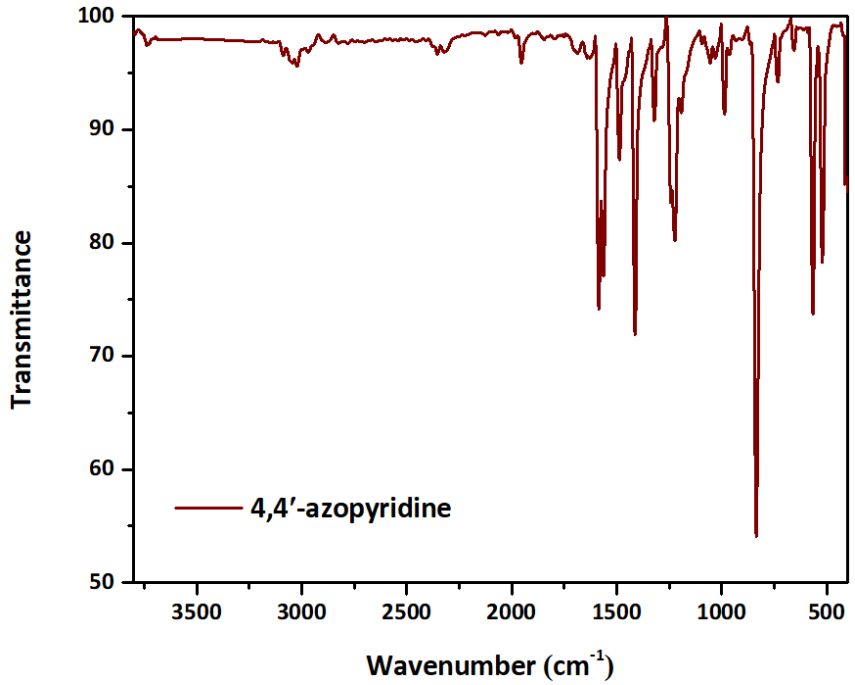

(c)

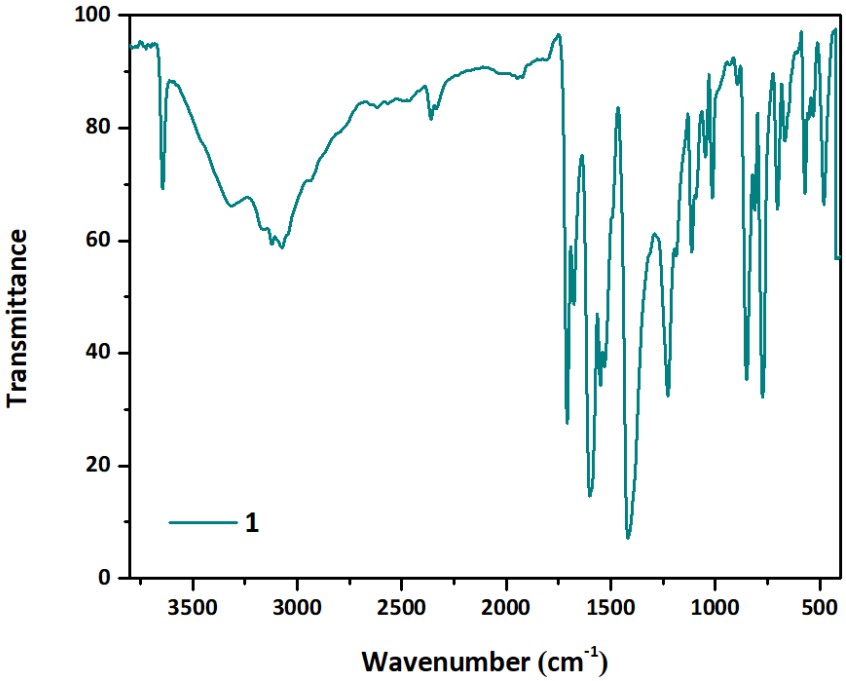

Fig. S4 FT-IR spectra of (a) BTB, (b) 4,4’-azopyridine and (c) **1**.

E. Powder XRD pattern

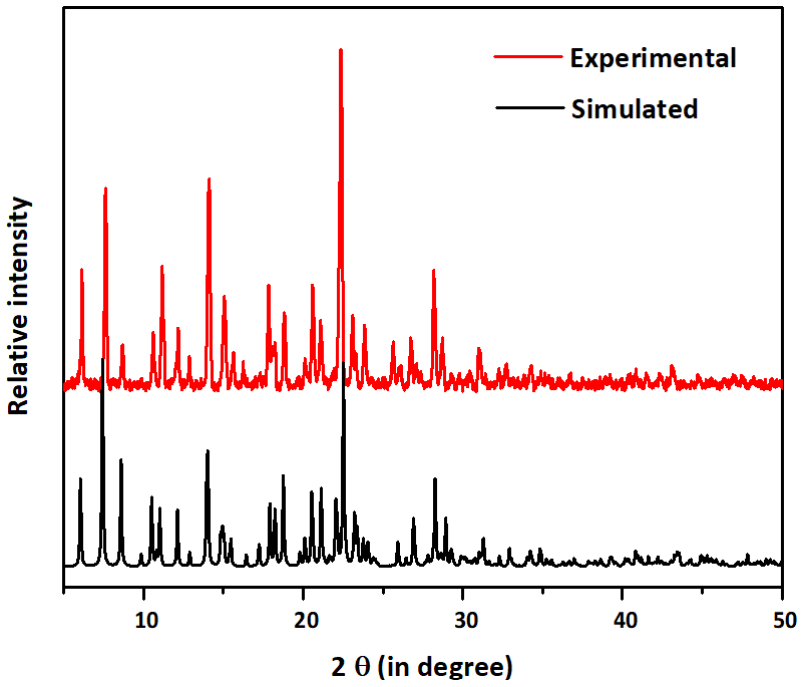

Fig. S5 PXRD pattern of simulated and as-synthesized **1**.

F. Thermogravimetric analysis

(a)

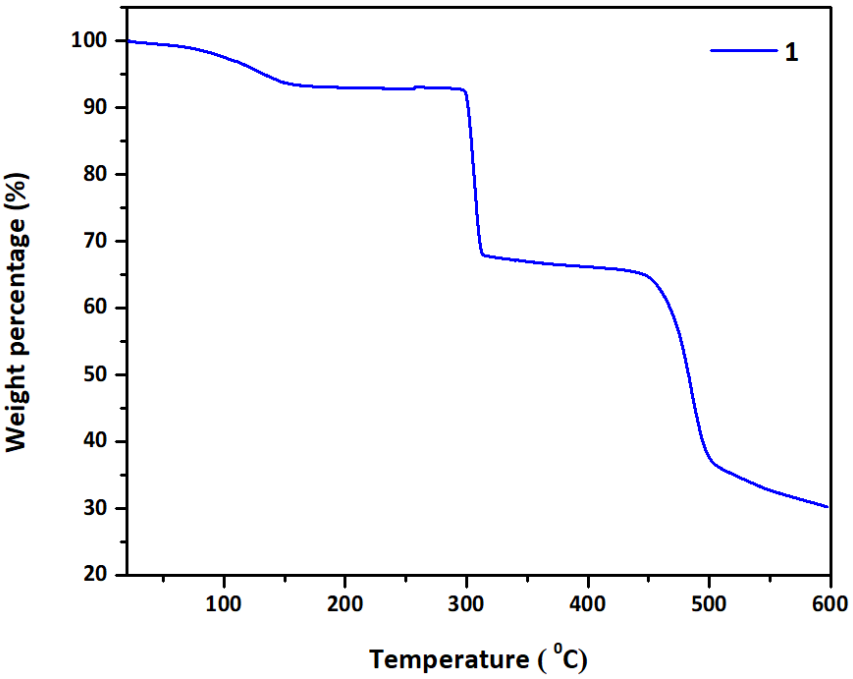

(b)

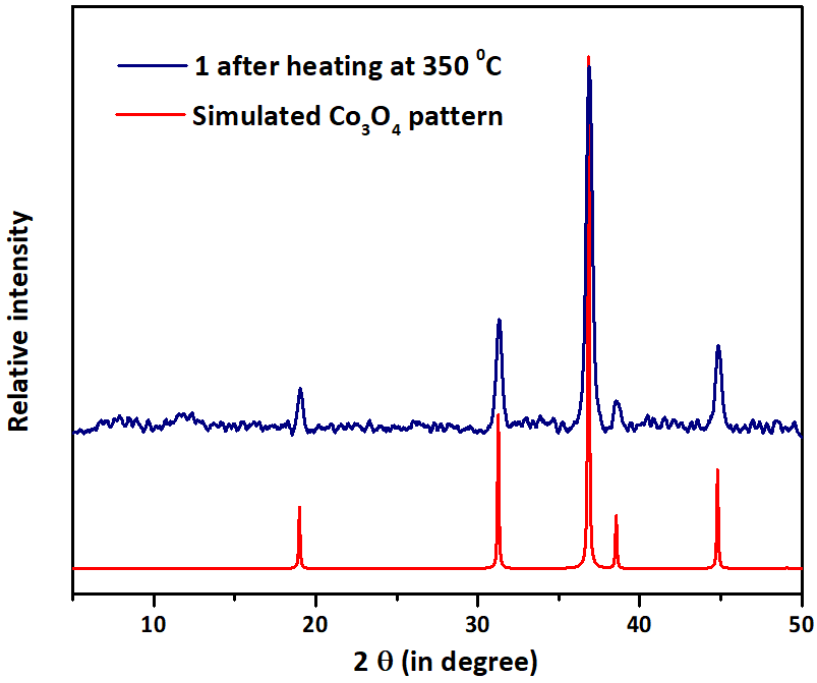

Fig. S6 (a) Thermogravimetric analysis shows the thermal stability of **1** up to 295 ^{0}C, (b) PXRD confirms the formation of Co_3O_4 after framework destruction at 350 ^{0}C.[S21]

G. Steady-state spectroscopy

UV-Vis absorption spectra

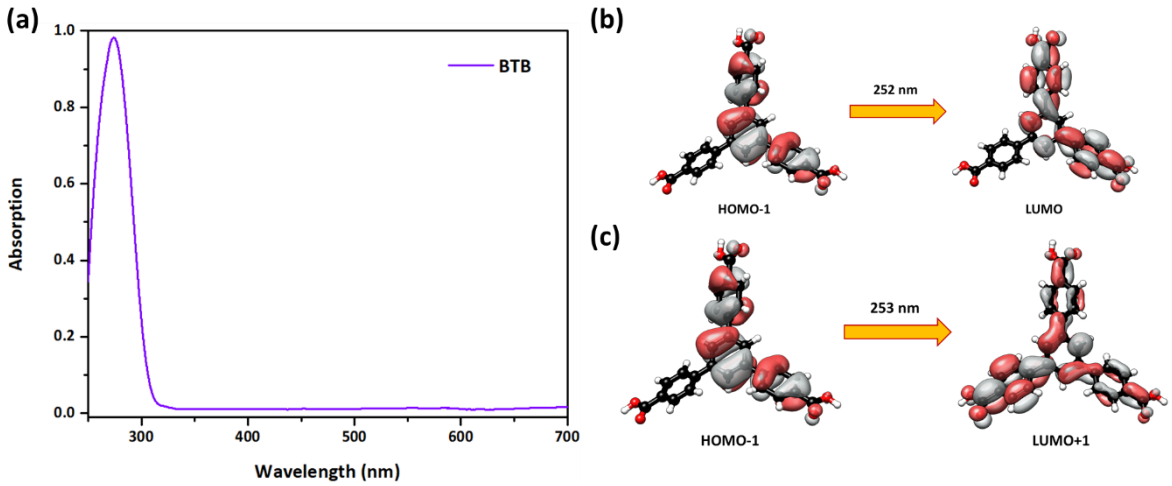

Fig. S7 (a) UV-Vis absorption spectrum of BTB, and (b, c) pictorial representation of corresponding molecular orbitals associated to the electronic transitions.

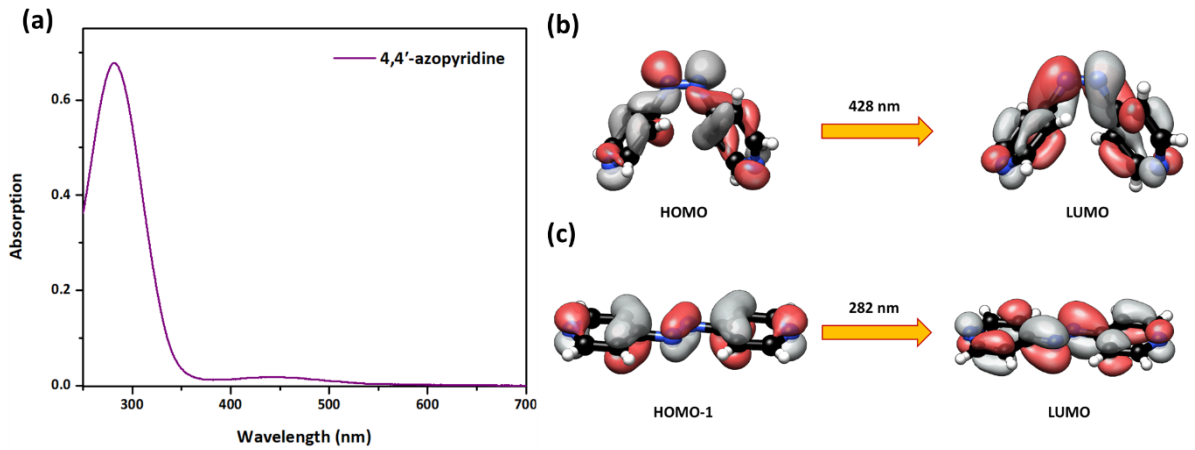

Fig. S8 (a) UV-Vis absorption spectrum of 4,4'-azopyridine, pictorial representation of corresponding molecular orbitals of (b) *trans*- and (c) *cis*-conformer associated to these electronic transitions.

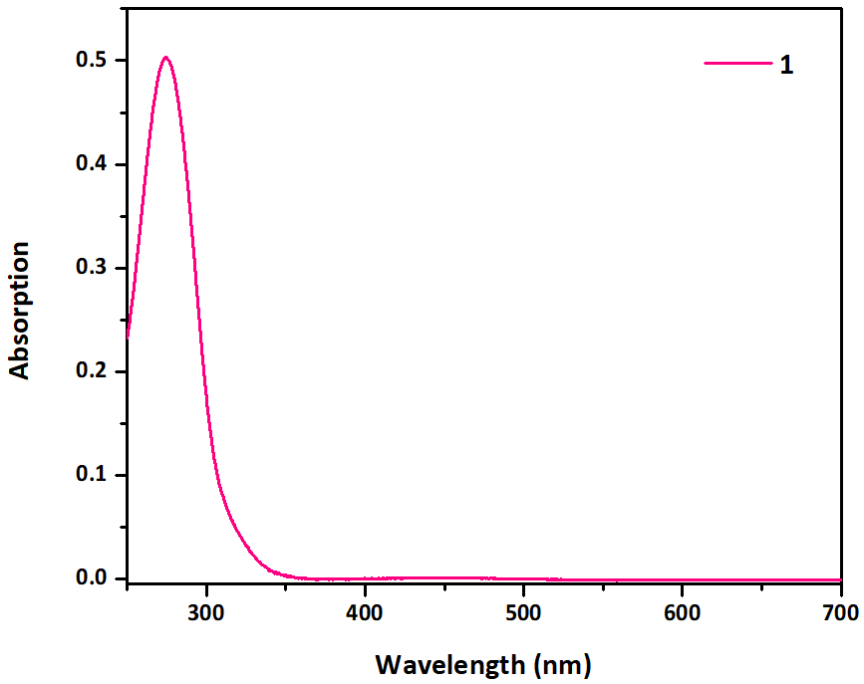

Fig. S9 UV-Vis absorption spectrum of **1**.

Emission spectra

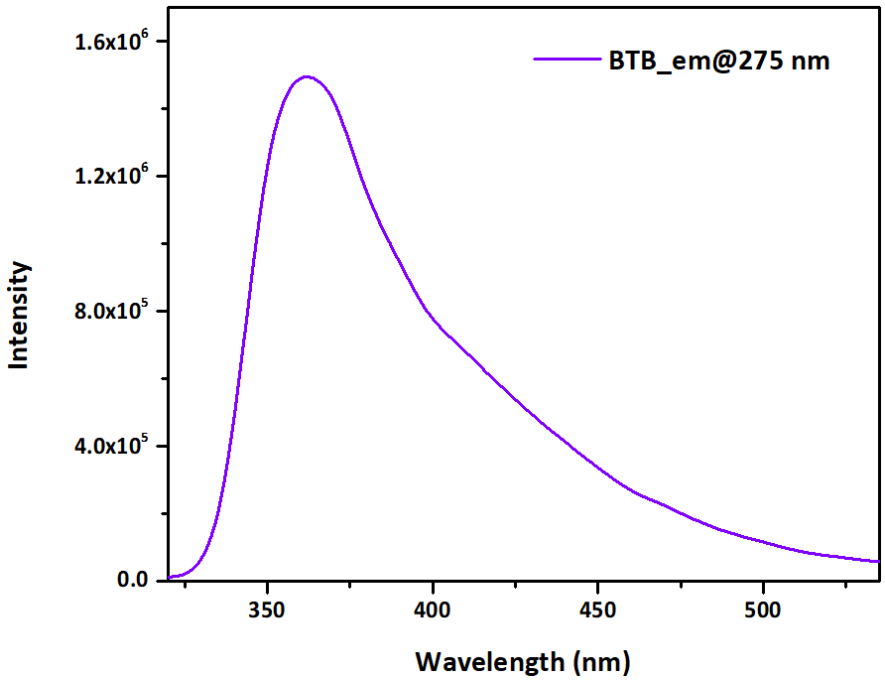

Fig. S10 Emission spectra of BTB (excitation at 275 nm).

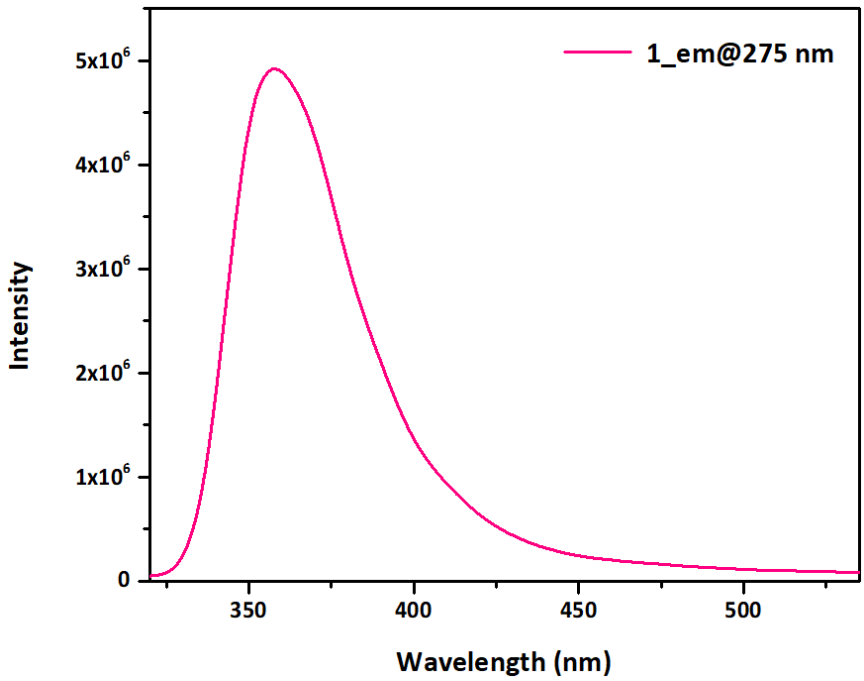

Fig. S11 Emission spectra of **1** (excitation at 275 nm).

Excitation spectra

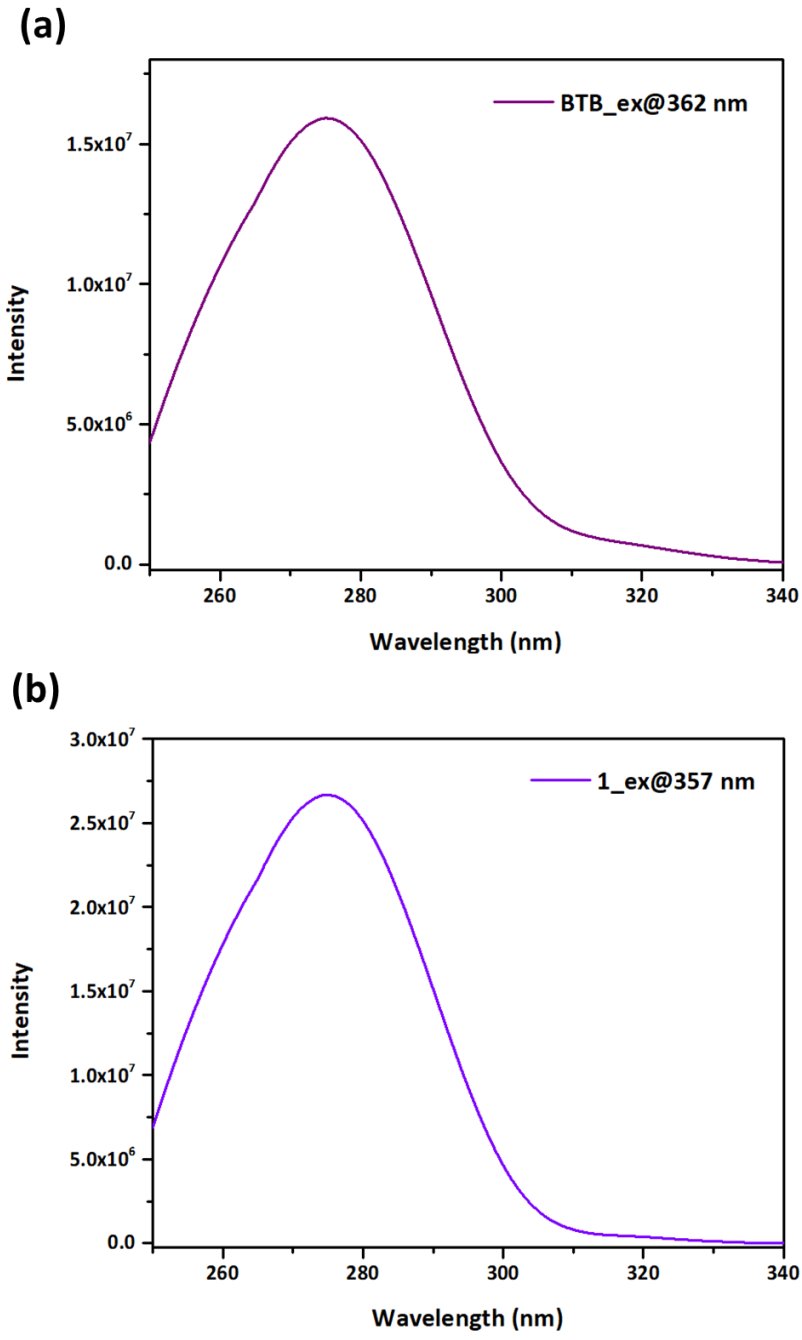

Fig. S12 Excitation spectra of the (a) BTB and (b) **1**.

H. Fluorescence lifetime decay profile of BTB and 1

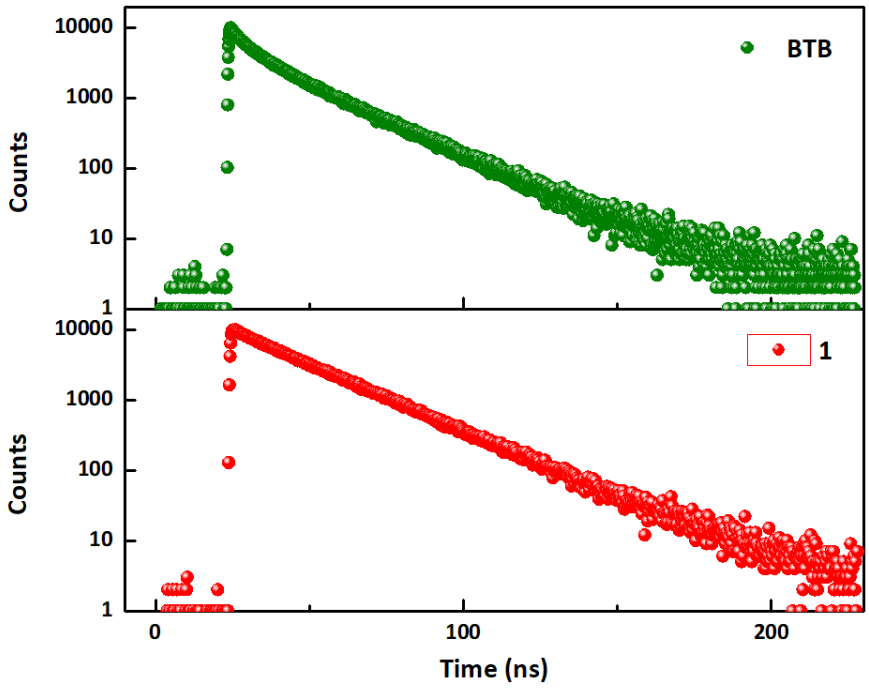

Fig. S13 The lifetime decay profile of (a) BTB and (b) **1** (λ_{ex} = 310 nm; λ_{probe} = 357 nm).

Table S5. Detail parameters of the fitted fluorescence decay plot of BTB in water.

λ excitation	λ detection	α_1	τ_1 (ns)	α_2	τ_2 (ns)	χ_2
310 nm	357 nm	0.19	5.243	0.81	21.114	1.14

Table S6. Detail parameters of the fitted fluorescence decay plot of **1** in water.

λ excitation	λ detection	α_1	τ_1 (ns)	α_2	τ_2 (ns)	χ_2
310 nm	357 nm	0.02	5.769	0.98	22.883	1.11

I. Stability test in water

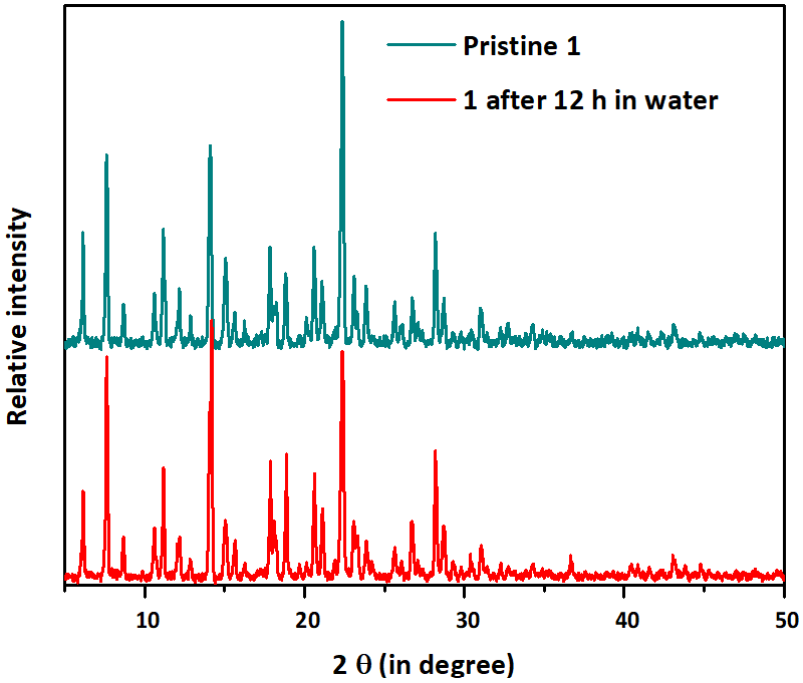

Fig. S14 PXRD of the **1** before and after kept in water for 12 h.

J. Faraday-Tyndall experiment and DLS study

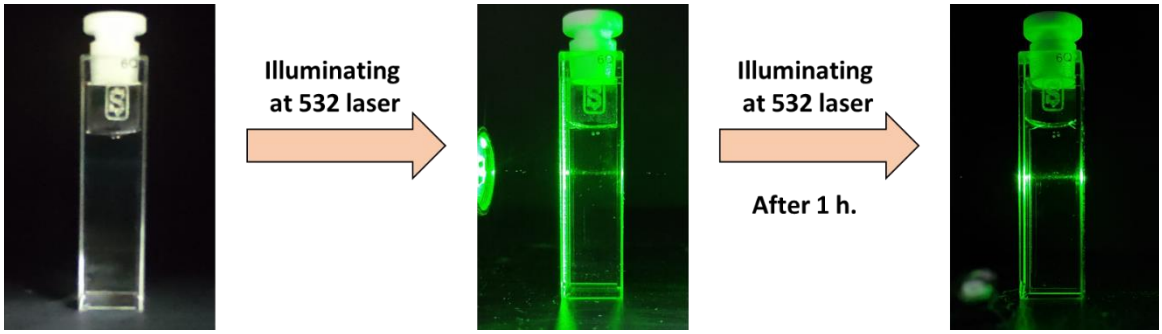

Fig. S15 Faraday-Tyndall effect showing uniform dispersibility of the solution and also after 1 h.

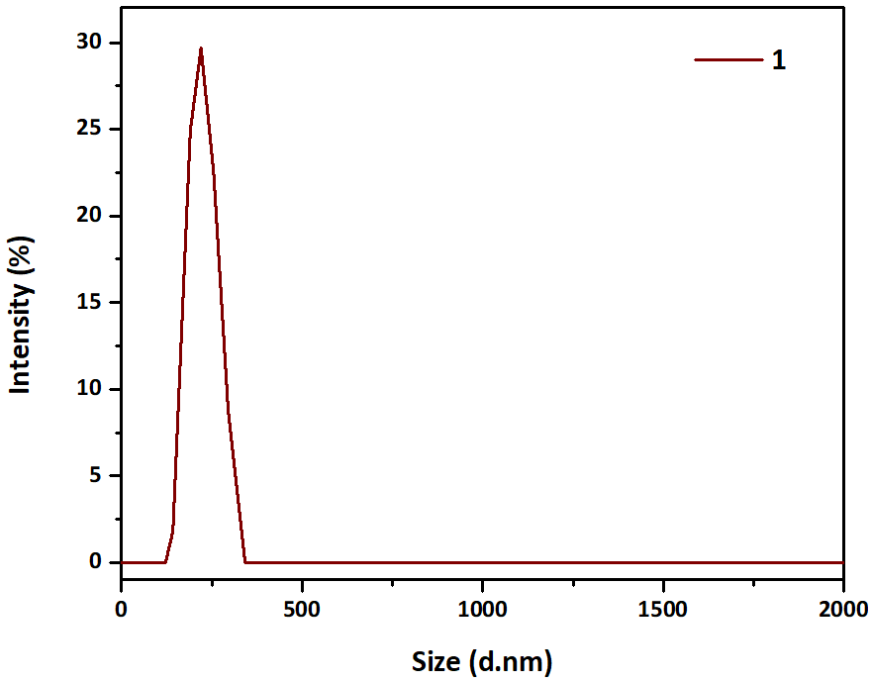

Fig. S16 Dynamic light scattering (DLS) study showing uniformly dispersed **1** particle in water with an average particle diameter of 219 nm.

K. Limit of detection calculation for Pb (II) ion

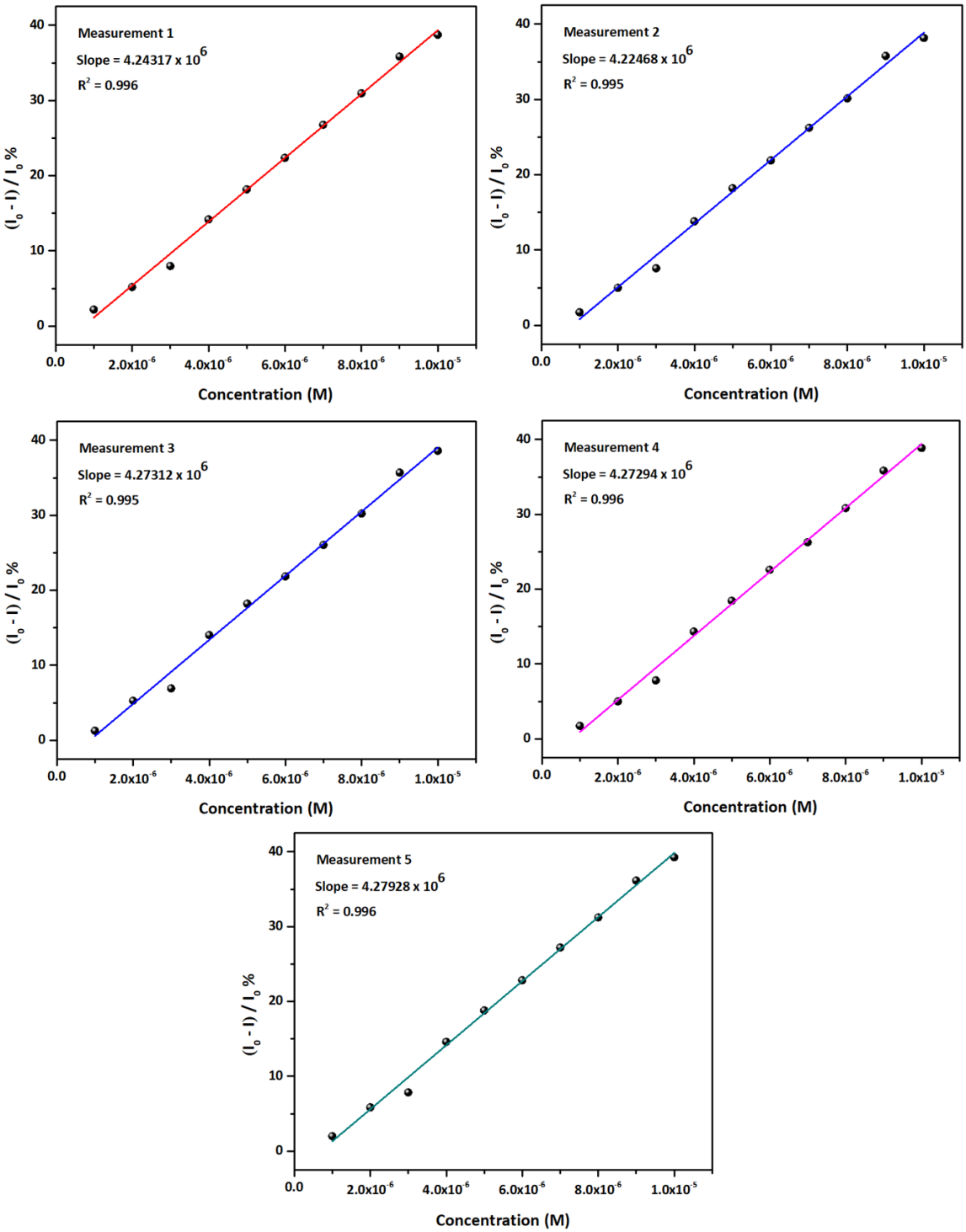

Fig. S17 Emission quenching ratio (at 357 nm) with respect to Pb (II) concentration fitted in a linear relationship to obtain the slope for limit of detection (LOD) calculation.

L. Recyclability tests

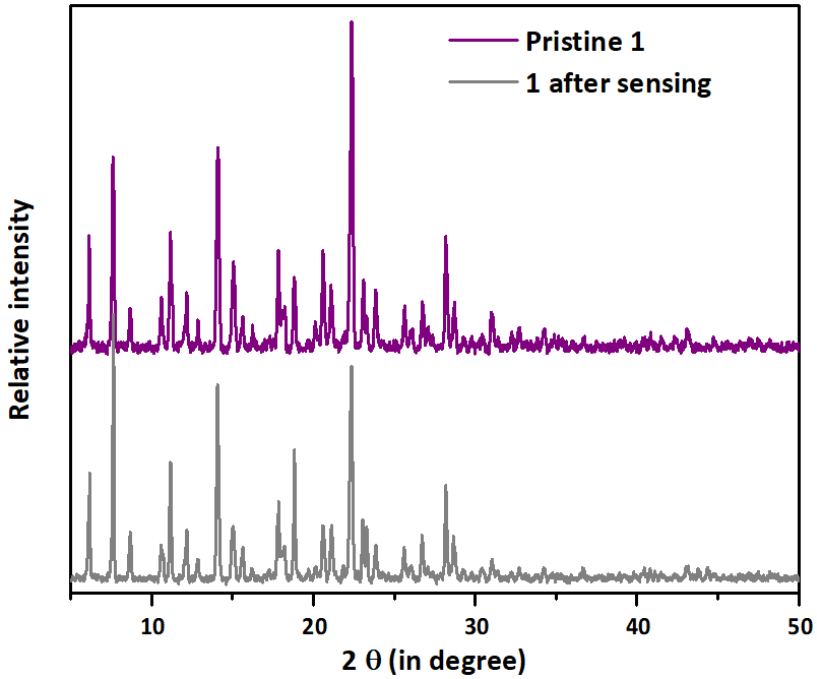

Fig. S18 PXRD of **1** before and after Pb (II) sensing.

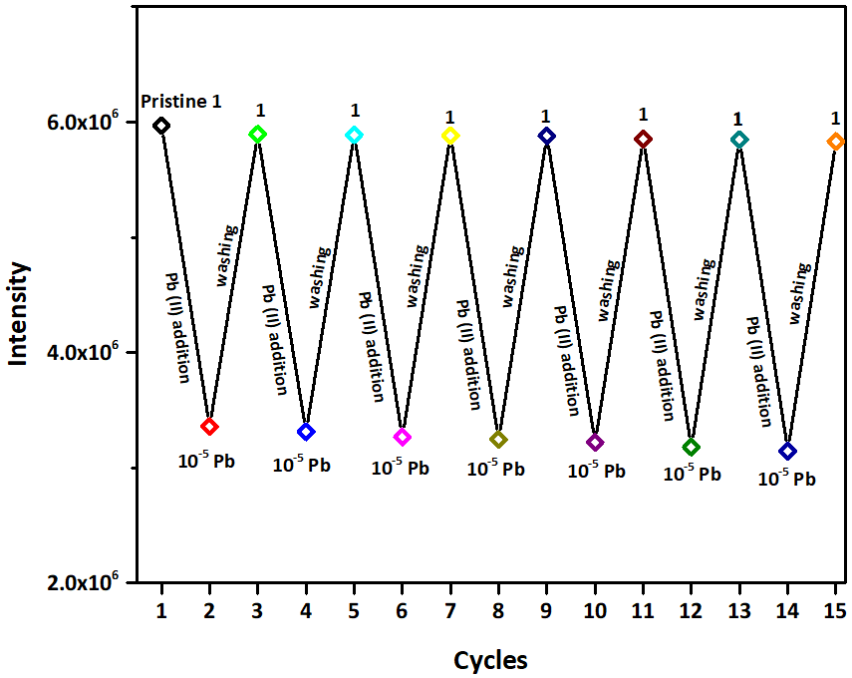

Fig. S19 Retention of emission intensity and quenching efficiency of **1** upon Pb (II) sensing and being washed with water in alternative cycles.

M. Sensing at different pH

(a)

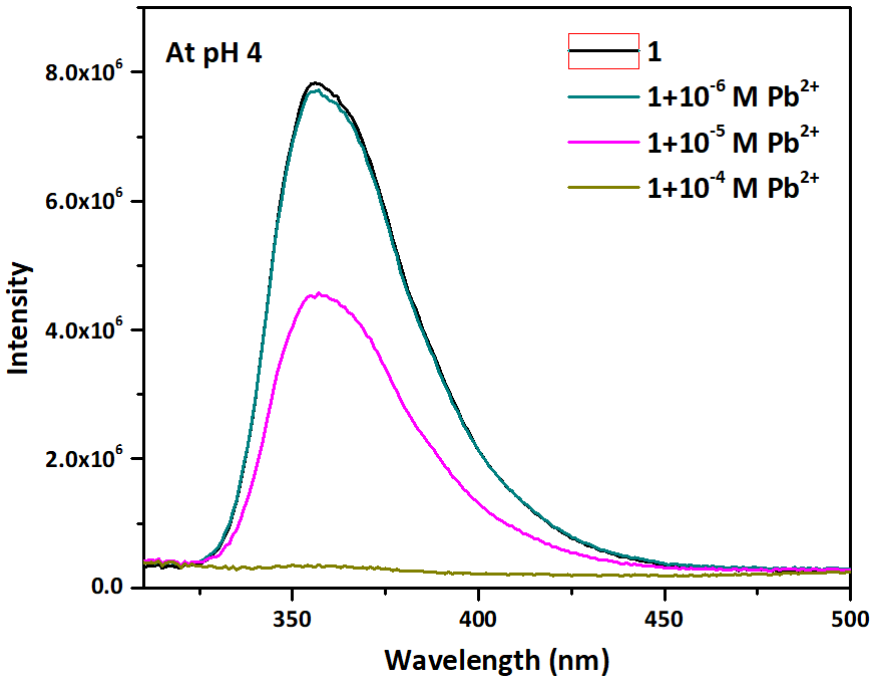

(b)

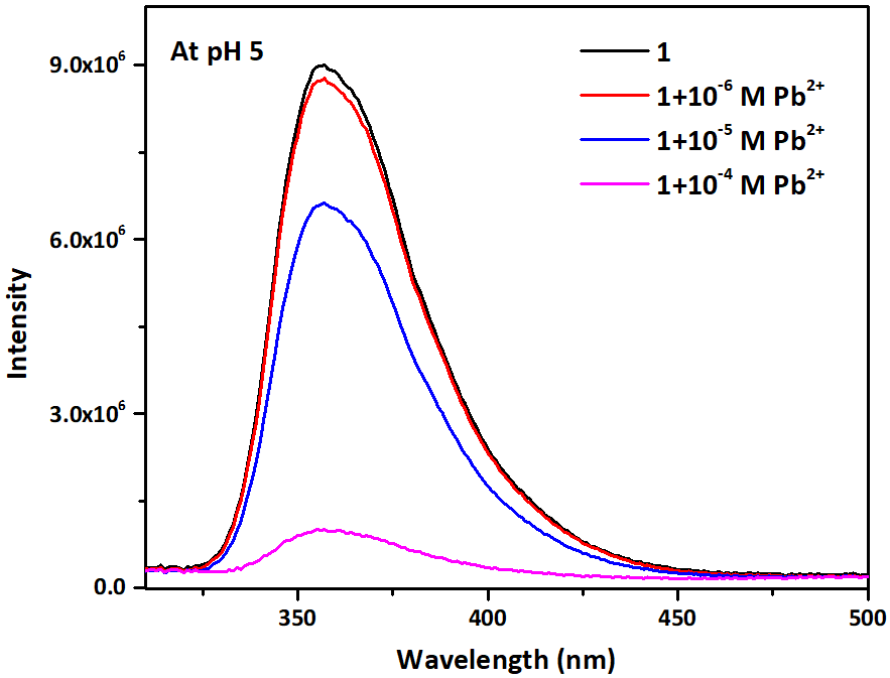

(c)

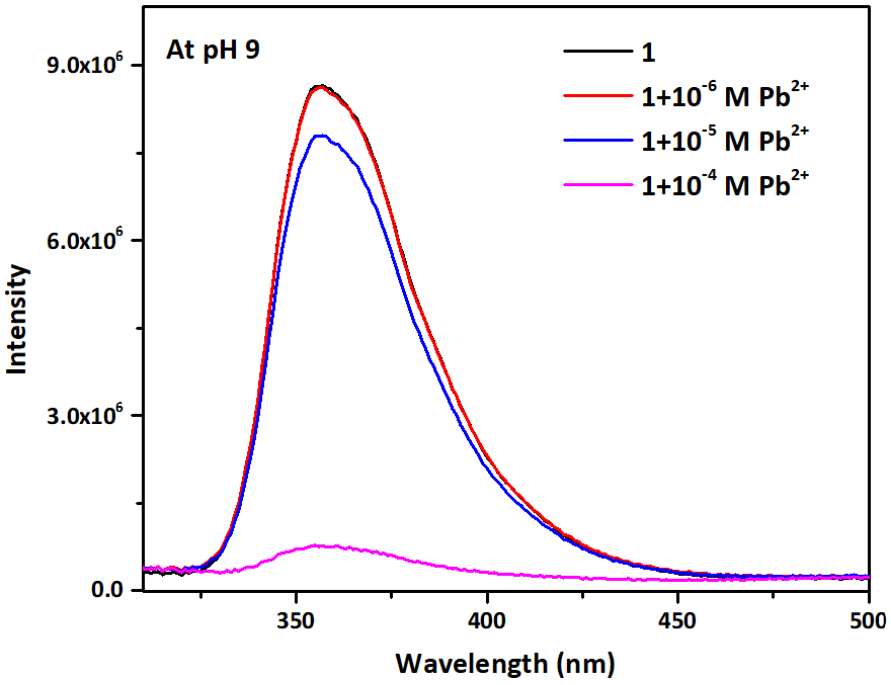

Fig. S20 Pb (II) sensing at different pH of the reaction medium.

N. Spiking

Table S7. Pb (II) spiking from natural water resources.

Water resources	Added Pb (II) concentration (M)	Detected Pb (II) concentration (µM)
River water	10^{-5}	1.2×10^{-5}
	10^{-6}	10^{-6}
Drinking water	10^{-5}	1.1×10^{-5}
	10^{-6}	10^{-6}
Tap water	10^{-5}	10^{-5}
	10^{-6}	0.9×10^{-6}

O. Absorption spectra of 1 with different Pb (II) ion concentrations

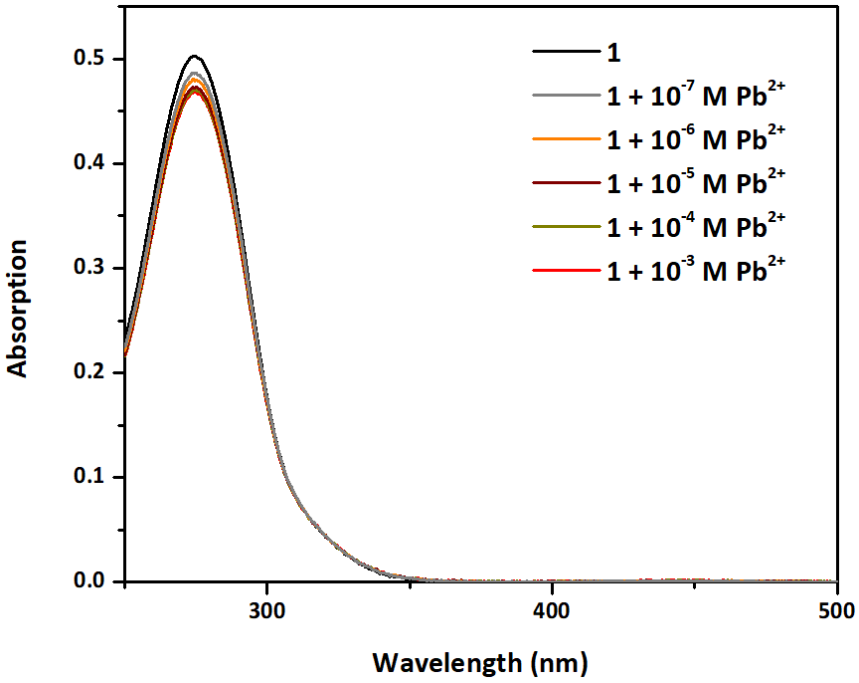

Fig. S21 Absorption spectra of **1** in pristine state and after adding Pb (II) in increasing concentrations.

P. Table S8. Detail parameters of the fitted fluorescence decay plot of **1** after adding $PbCl_2$ aqueous solution.

$\lambda_{excitation}$	$\lambda_{detection}$	α_1	τ_1 (ns)	α_2	τ_2 (ns)	α_3	τ_3 (ns)	χ_2
310 nm	357 nm	0.10	0.489	0.03	5.978	0.87	22.606	0.97

Q. Stern-Volmer plots

(a)

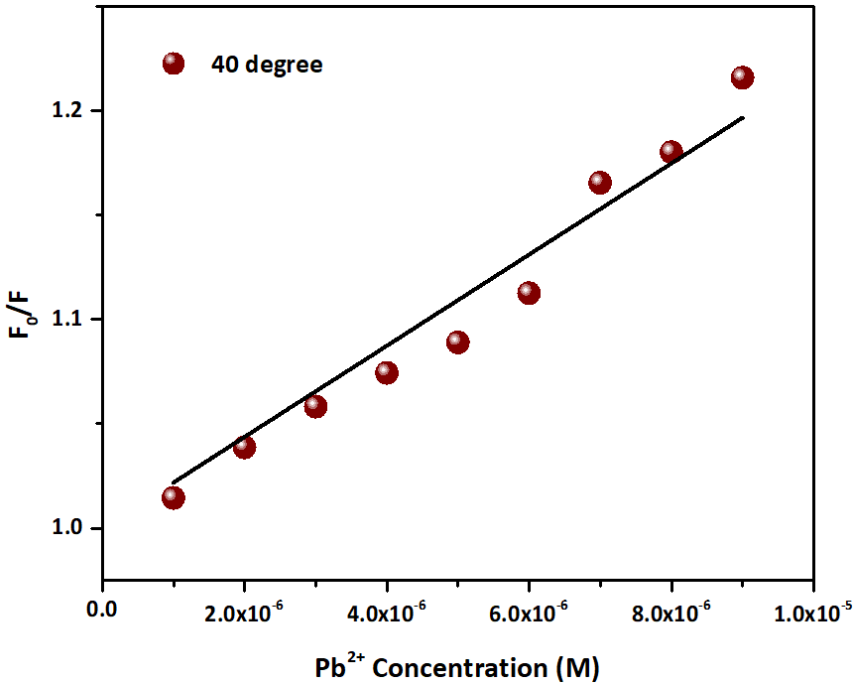

(b)

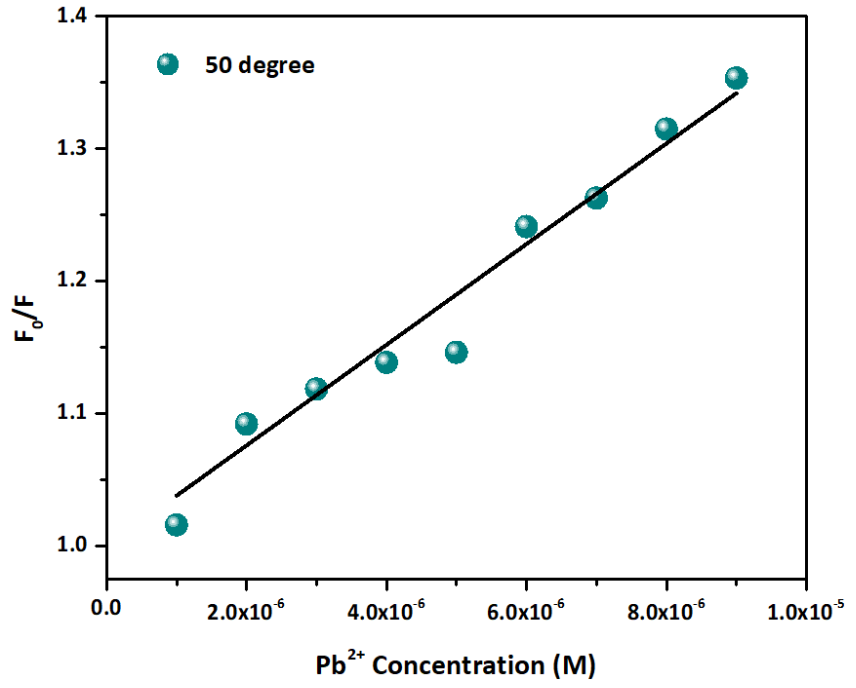

Fig. S22 The Stern-Volmer plots of **1** at two different temperatures.

R. Host-guest interaction

We optimized the possible orientations (named as adduct 1-6 as Figs. 5 and S23-S27, respectively) of $PbCl_2$ over the BTB molecule, (a) one $PbCl_2$ molecule on each individual peripheral benzene moiety (Figs. 5, S23-S24), (b) one $PbCl_2$ molecule on central benzene moiety (Fig. S25), (c) two $PbCl_2$ molecules on two peripheral benzene moieties (Fig. S26), (d) two $PbCl_2$ molecules on central benzene moiety (Fig. S27).

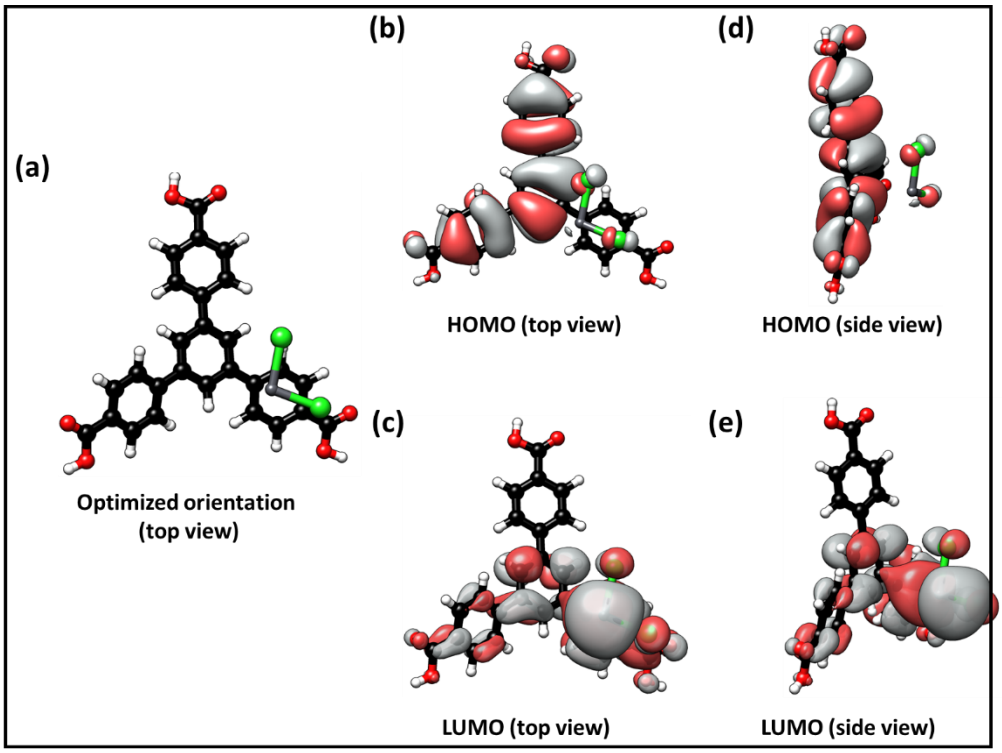

Fig. S23 Adduct 2: (a) Optimized $PbCl_2$ position on BTB molecule (peripheral benzene moiety), their corresponding HOMO (b: top view, c: side view) and LUMO (d: top view, e: side view).

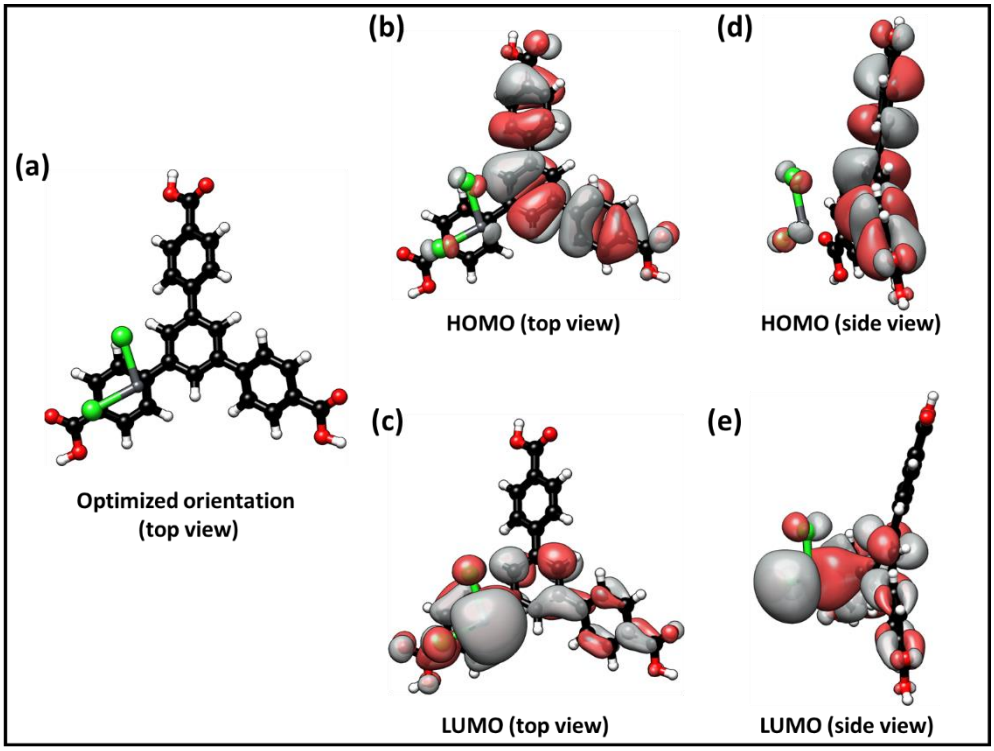

Fig. S24 Adduct 3:(a) Optimized $PbCl_2$ position on BTB molecule (peripheral benzene moiety), their corresponding HOMO (b: top view, c: side view) and LUMO (d: top view, e: side view).

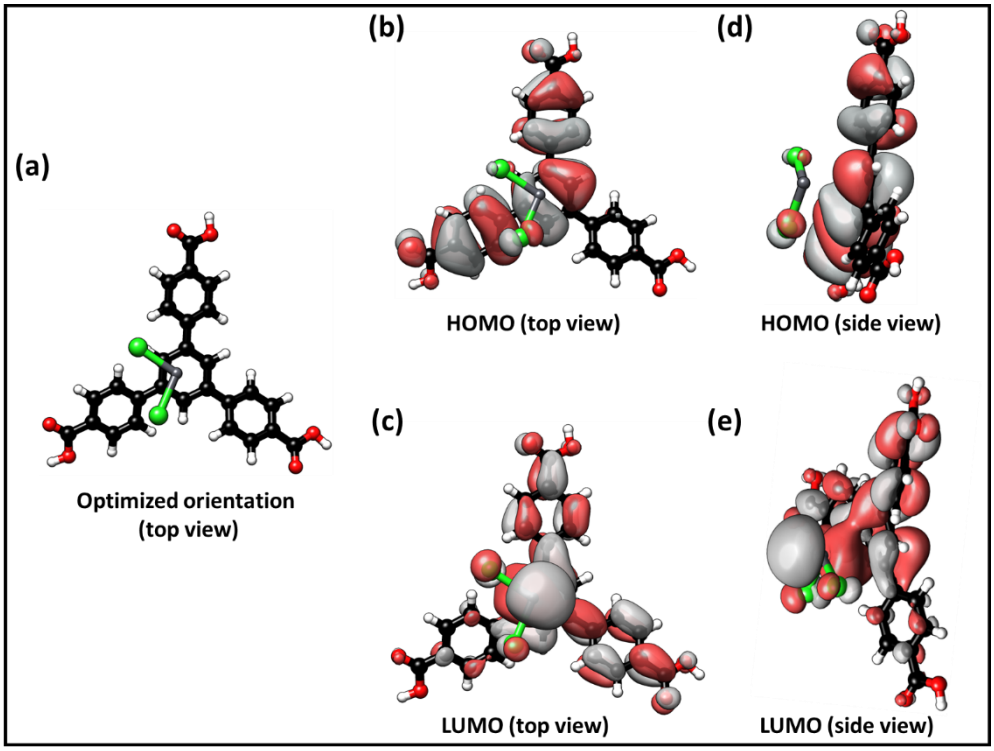

Fig. S25 Adduct 4: (a) Optimized $PbCl_2$ position on BTB molecule (central benzene moiety), their corresponding HOMO (b: top view, c: side view) and LUMO (d: top view, e: side view).

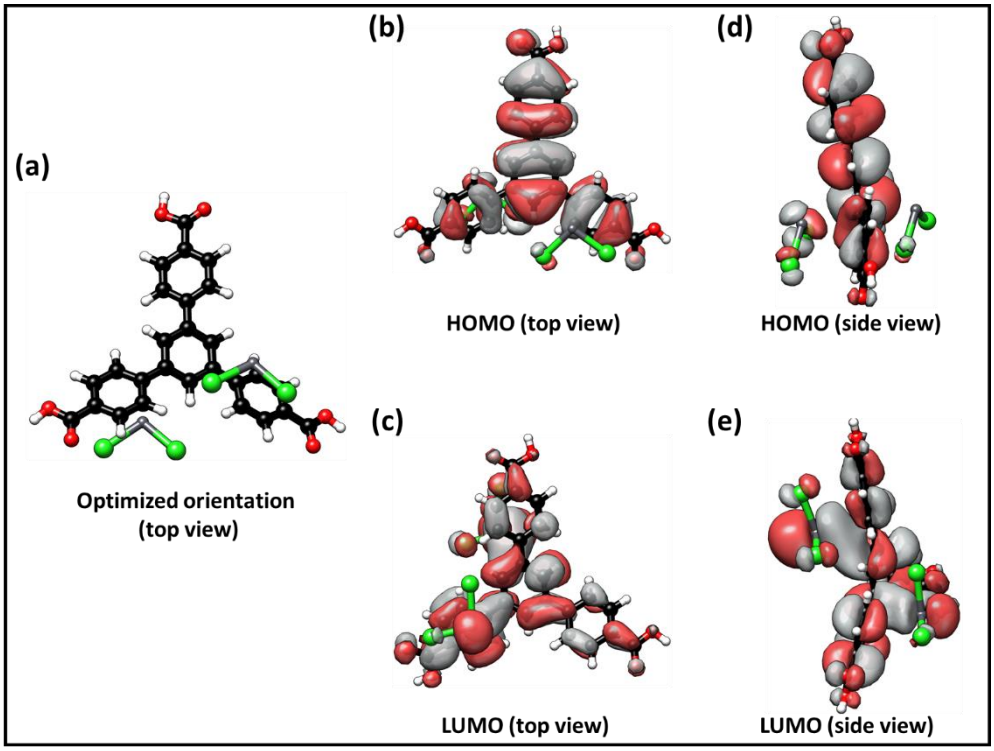

Fig. S26 Adduct 5: (a) Optimized $PbCl_2$ position on BTB molecule (two $PbCl_2$ molecules each on two peripheral benzene moieties), their corresponding HOMO (b: top view, c: side view) and LUMO (d: top view, e: side view).

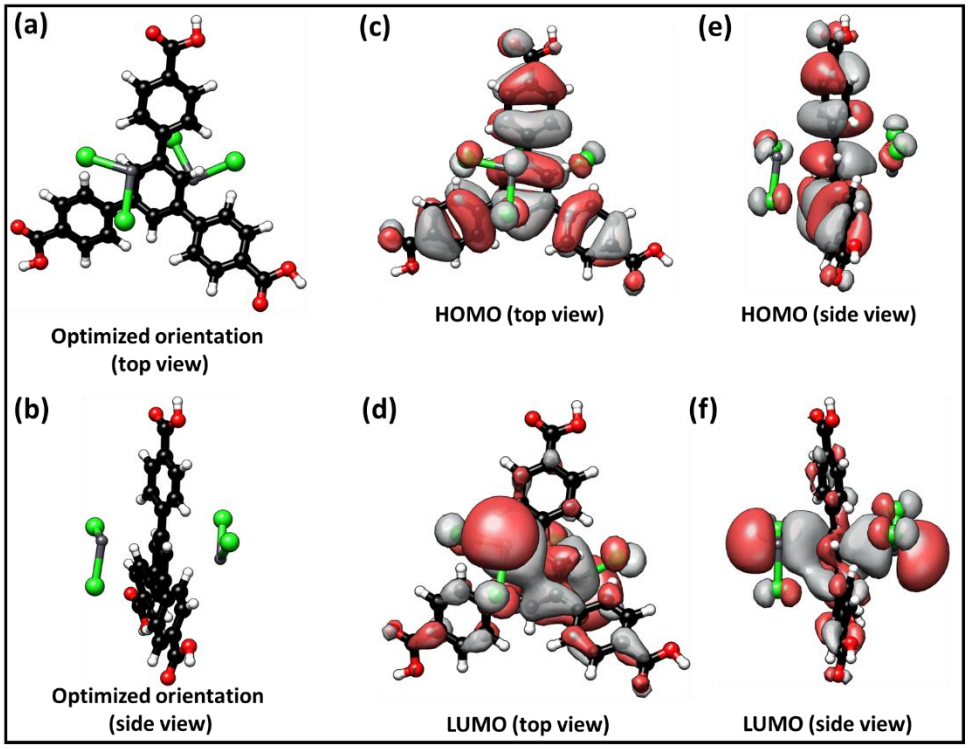

Fig. S27 Adduct 6: (a) Optimized $PbCl_2$ position on BTB molecule (two $PbCl_2$ molecules on central benzene moieties), their corresponding HOMO (b: top view, c: side view) and LUMO (d: top view, e: side view).

Table S9. Stabilization energy of optimized $PbCl_2$ on BTB molecule.

Adduct No.	**Stabilization Energy (eV) per $PbCl_2$**
Adduct 1 (Figure 5)	0.579
Adduct 2 (Figure S20)	0.584
Adduct 3 (Figure S21)	0.563
Adduct 4 (Figure S22)	0.759
Adduct 5 (Figure S23)	0.593
Adduct 6 (Figure S24)	0.734

S. Limit of detection calculation for Hg (II) ion

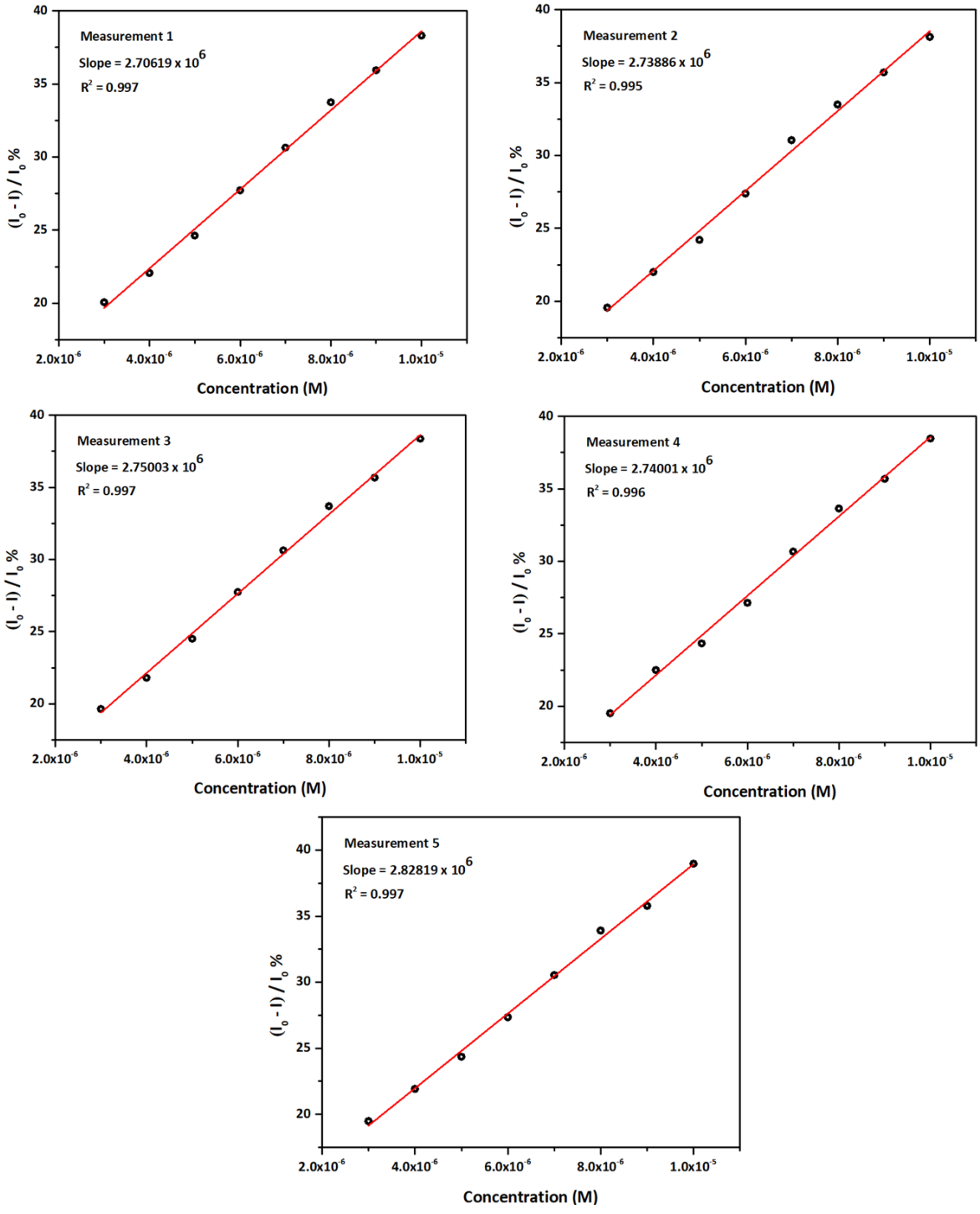

Fig. S28 Emission quenching ratio (at 357 nm) with respect to Hg (II) concentration fitted in a linear relationship to obtain the slope for limit of detection (LOD) calculation.

T. Anti-inference ability of 1 for Hg (II) sensing and comparison

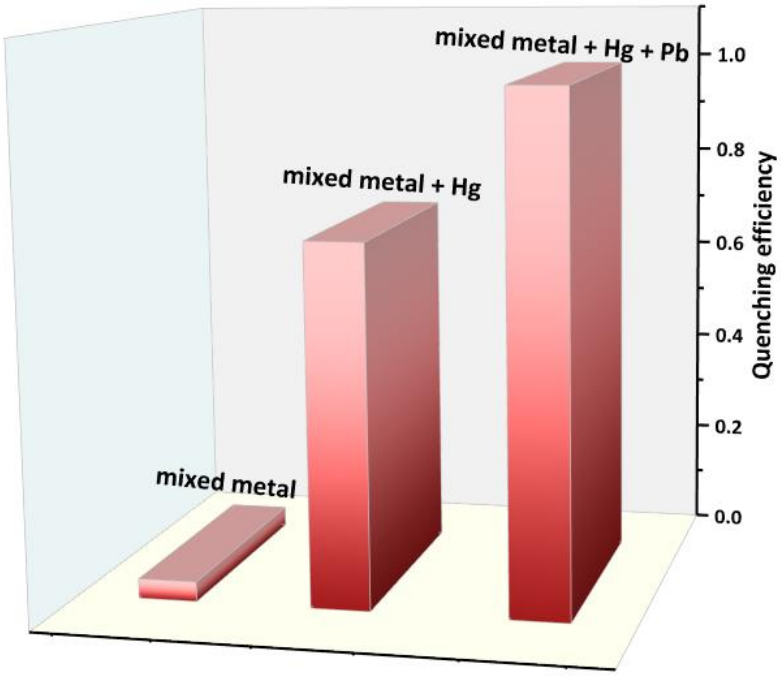

Fig. S29 Selective sensing of Hg (II) in presence of mixed metal ions (middle bar), whereas right bar shows more sensing efficiency of Pb (II) in presence of all metal ions and Hg (II) ions in the aqueous solution.

U. Absorption spectra of 1 with different Hg (II) ion concentrations

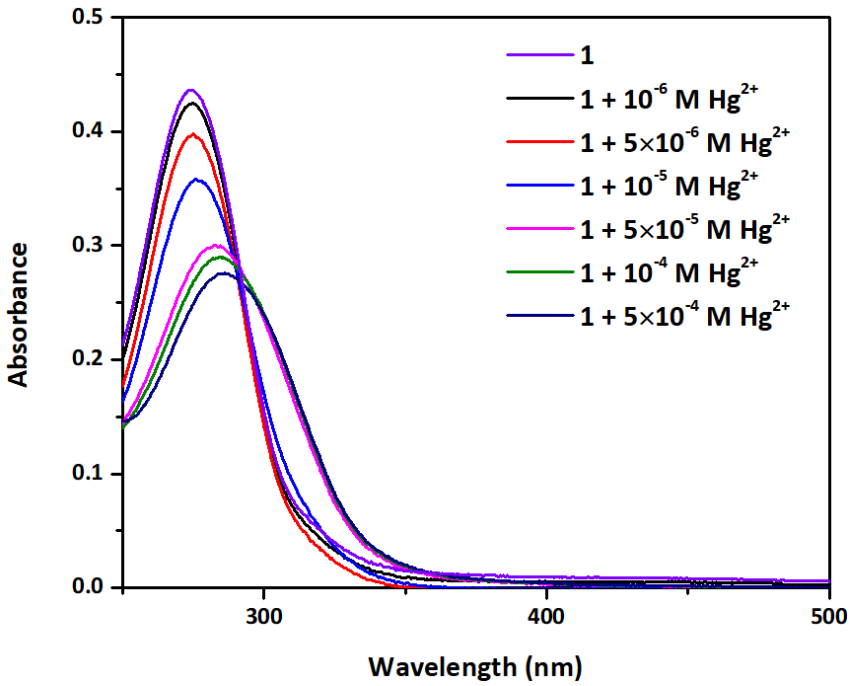

Fig. S30 Absorption spectra of **1** in pristine state and after adding Hg (II) with increasing concentrations.

V. XPS spectra

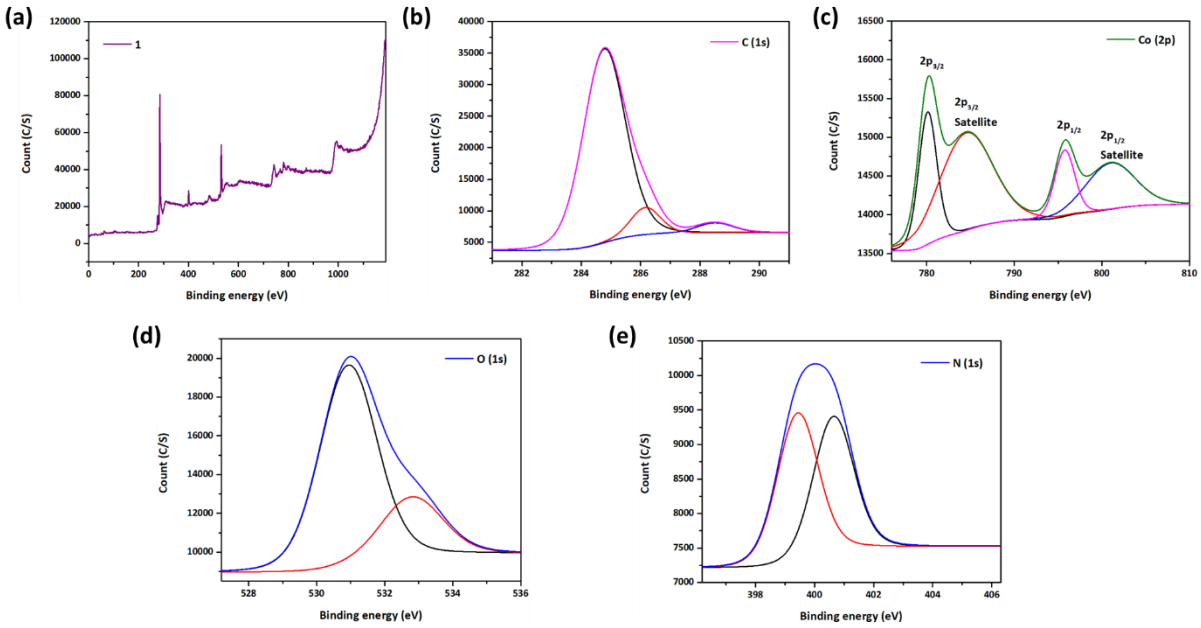

Fig. S31 XPS spectra of pristine **1**: (a) survey, (b) C 1s, (c) Co 2p, (d) O 1s, (e) N 1s spectrum.

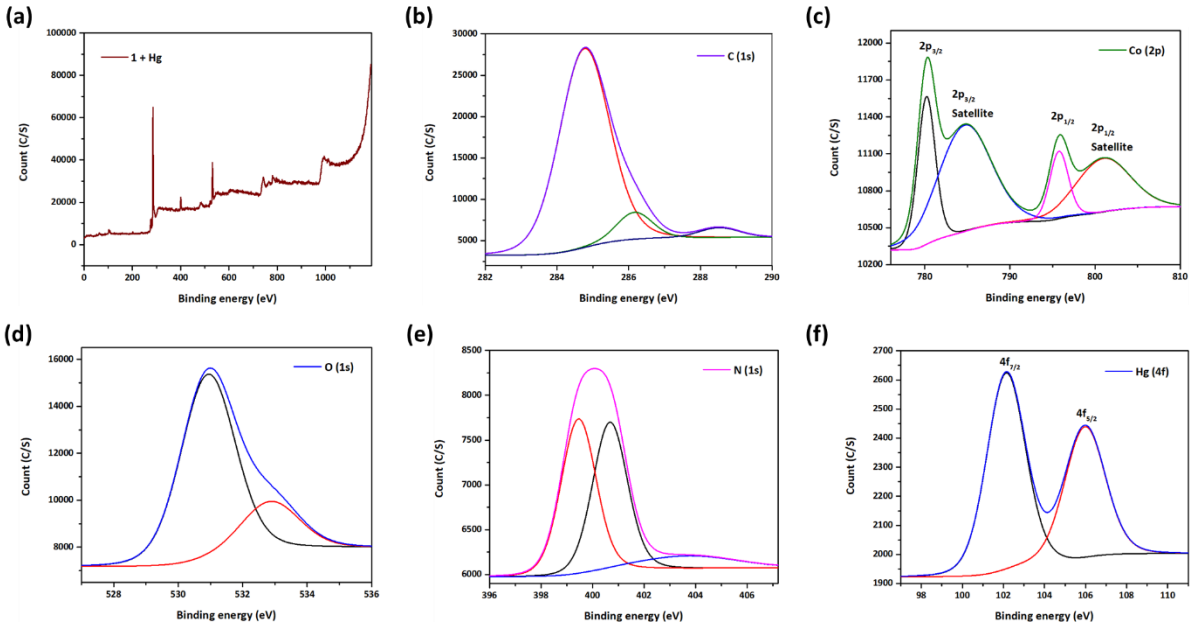

Fig. S32 XPS spectra of pristine **1** after addition of Hg (II) solution: (a) survey, (b) C 1s, (c) Co 2p, (d) O 1s, (e) N 1s, (f) Hg 4f spectrum.

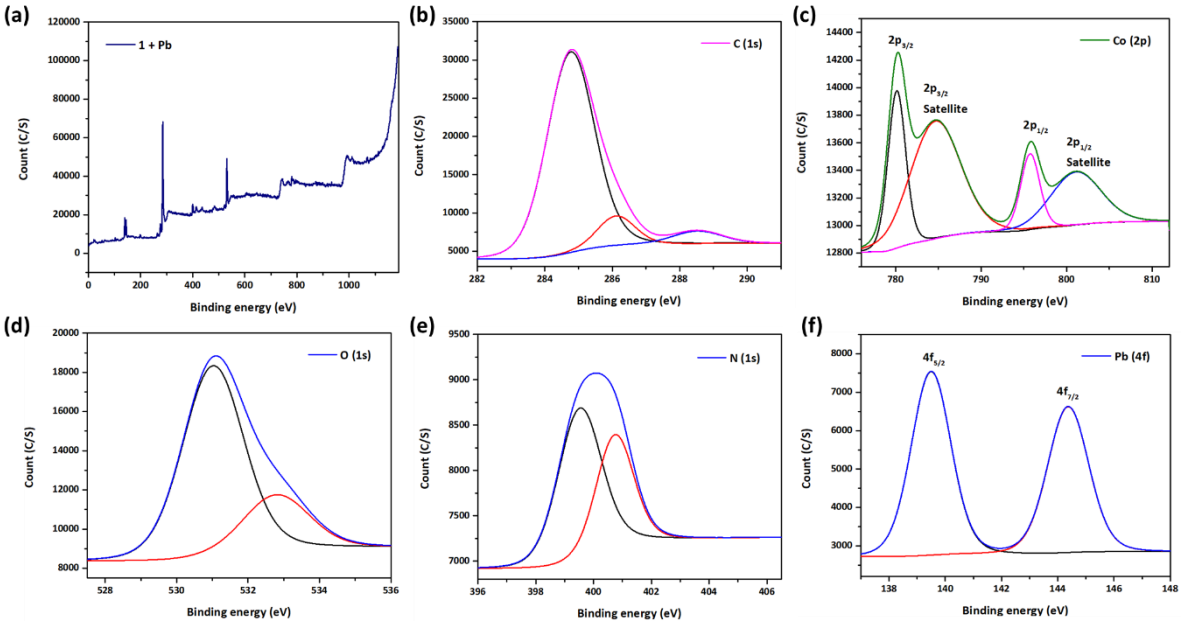

Fig. S33 XPS spectra of pristine **1** after addition of Pb (II) solution: (a) survey, (b) C 1s, (c) Co 2p, (d) O 1s, (e) N 1s, (f) Pb 4f spectrum.

W. Fluorescence lifetime decay profile of 1 after addition of $HgCl_2$ solution

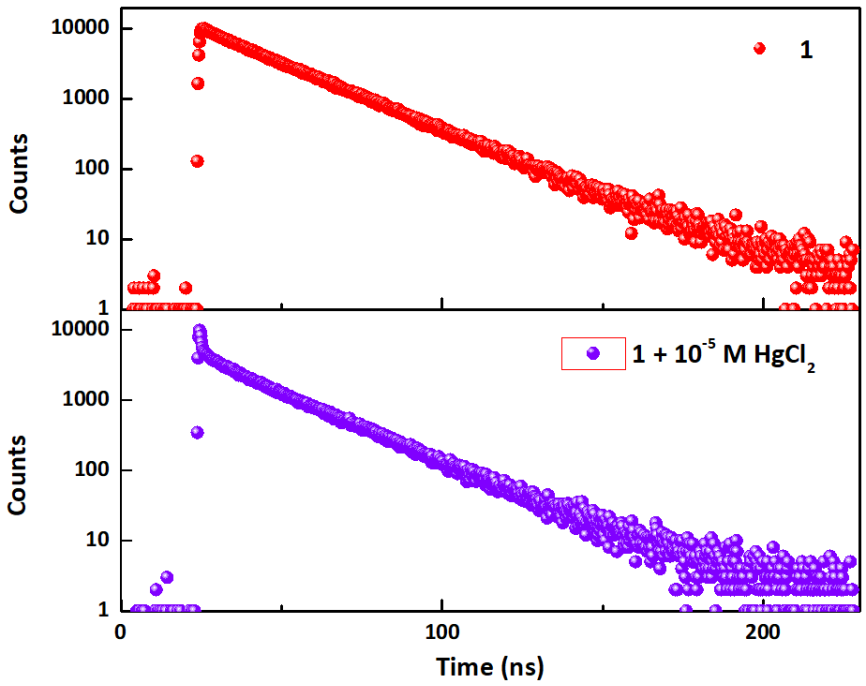

Fig. S34 The comparative lifetime decay profile of (a) **1**, and (b) after addition of Hg (II) solution (λ_{ex} = 310 nm; λ_{probe} = 357 nm).

Table S10. Lifetime decay profile of **1** after addition of $HgCl_2$ aqueous solution.

λ excitation	λ detection	α_1	τ_1 (ns)	α_2	τ_2 (ns)	α_3	τ_3 (ns)	χ_2
310 nm	357 nm	0.06	0.3	0.07	5.563	0.87	22.216	0.97

X. References

S1 L. Li, Q. Chen, Z. Niu, X. Zhou, T. Yang and W. Huang, *J. Mater. Chem. C*, 2016, **4**, 1900–1905.

S2 K. Yi and L. Zhang, *J. Hazard. Mater.*, 2020, **389**, 122141.

S3 Z. Li, Z. Zhan and M. Hu, *CrystEngComm*, 2020, **22**, 6727–6737.

S4 G. Ji, J. Liu, X. Gao, W. Sun, J. Wang, S. Zhao and Z. Liu, *J. Mater. Chem. A*, 2017, **5**, 10200–10205.

S5 X. An, Q. Tan, S. Pan, H. Liu and X. Hu, *Spectrochim. Acta Part A Mol. Biomol. Spectrosc.*, 2021, **247**, 119073.

S6 L. H. Chen, X. Bin Cai, Q. Li, B. Bin Guan, T. H. Liu, D. Li, Z. Q. Wu and W. Zhu, *J. Solid State Chem.*, 2021, **302**, 122416.

S7 J.-X. Hou, J.-P. Gao, J. Liu, X. Jing, L.-J. Li and J.-L. Du, *Dye. Pigment.*, 2019, **160**, 159–164.

S8 S. Xu, L. Zhan, C. Hong, X. Chen, X. Chen and M. Oyama, *Sensors Actuators B Chem.*, 2020, **308**, 127733.

S9 D.-C. Hu, X.-R. Da, J.-J. Tan, X.-F. Guo, H. Feng and J.-C. Liu, *Polyhedron*, 2020, **186**, 114613.

S10 Q. Li, B.-B. Guan, W. Zhu, T.-H. Liu, L.-H. Chen, Y. Wang and D.-X. Xue, *J. Solid State Chem.*, 2020, **291**, 121672.

S11 Rigaku Oxford Diffraction. CrysAlisPro Software System, version 1.171.39.30d, Rigaku Corporation: Oxford, UK, 2018.

S12 G. M. Sheldrick, Crystal Structure Refinement with SHELXL. *Acta Crystallogr., Sect. C: Struct. Chem.* 2015, **71**, 3–8.

S13 O. V. Dolomanov, L. J. Bourhis, R. J. Gildea,Howard, J. A. Gildea, H. Puschmann, *J. Appl. Crystallogr*. 2009, **42**, 339−341.

S14 A. Nath, S. Chawla, A. K. De, P. Deria, S. Mandal, *Chem. Eur. J*. 2022, accepted.

S15 I. B. Berlman, "Handbook of Fluorescence Spectra of Aromatic Molecules," *Academic Press* 1971, New York, N. Y.

S16 W. Liu, Y. Wang, Z. Bai, Y. Li, Y. Wang, L. Chen, L. Xu, J. Diwu, Z. Chai, S. Wang, *ACS Appl. Mater. Interfaces* 2017, **9**, 16448– 16457.

S17 J-D. Chaia, M. Head-Gordon, *Phys. Chem. Chem. Phys.* 2008, **10**, 6615-6620.

S18 P. J. Hay, W. R. Wadt, *J. Chem. Phys*. 1985, **82**, 270.

S19 P. J. Hay, W. R. Wadt, *J. Chem. Phys.* 1985, **82**, 299.

S20 M.J. Frisch, G.W. Trucks, H.B. Schlegel, G.E. Scuseria, M.A. Robb, J.R. Cheeseman, G. Scalmani, V. Barone, G. A. Petersson, H. Nakatsuji, X. Li, M. Caricato, A. V. Marenich, J. Bloino, B. G. Janesko, R. Gomperts, B. Mennucci, H, P, Hratchian, J. V. Ortiz, A. F. Izmaylov, J. L. Sonnenberg, D. Williams-Young, F. Ding, F. Lipparini, F. Egidi, J. Goings, B. Peng, A. Petrone, T. Henderson, D. Ranasinghe, V. G. Zakrzewski, J. Gao, N. Rega, G. Zheng, W. Liang, M. Hada, M, Ehara, K. Toyota, R. Fukuda, J. Hasegawa, M. Ishida, T. Nakajima, Y. Honda, O. Kitao, H. Nakai, T. Vreven, K. Throssell, J.A. Jr. Montgomery, J. E. Peralta, F. Ogliaro, M. J. Bearpark, J. J. Heyd, E. N. Brothers, K. N. Kudin, V. N. Staroverov, T. A. Keith, R. Kobayashi, J. Normand, K. Raghavachari, A. P. Rendell, J. C. Burant, S. S. Iyengar, J. Tomasi, M. Cossi, J. M. Millam, M, Klene, C. Adamo, R. Cammi, J. W. Ochterski, R. L. Martin, K. Morokuma, O. Farkas, J. B. Foresman, D. J. Fox, Gaussian 16 Revision C.01, Gaussian Inc., Wallingford CT 2016.

S21 D. D. M. Prabaharan, K. Sadaiyandi, M. Mahendran, S. Sagadevan, *Appl. Phys.* 2017, A **123**, 264.